Removal of Cr(VI) from wastewater by anionic clays

K. Ait Bentaleb[1], E. El Khattabi[2], M. Lakraimi[2*], L. Benaziz[2], E. Sabbar[1], M. Berraho[3], A. Legrouri[4]

[1]*Faculté des Sciences, Université Chouaib Doukkali, BP 20, El Jadida 24000, Morocco.*
[2]*Ecole Normale Supérieure, Université Cadi Ayyad, BP 2400, Marrakech 40000, Morocco.*
[3]*Faculté des Sciences Semlalia, Université Cadi Ayyad, BP 2390, Marrakech 40000, Morocco.*
[4]*International University of Grand-Bassam, Grand Bassam, Côte d'Ivoire.*

Abstract

Wastes containing chromium are considered hazardous because of their behavior in the deep soil layers when stored in landfills. In an alkaline medium, it is estimated that the stability of chromate can be 50 years; they can migrate to groundwater, even through cohesive soils. That is why we are interested in the elimination of chromium VI by a strong adsorbent such as one that belongs to the family of layered double hydroxides (anionic clays). These materials are synthesized by co-precipitation method at constant pH. The affinity of material for CrO_4^{2-} anion was studied as a function of contact time, pH of solution and mass ratio of [Zn-Al-Cl]/CrO_4. The removal of chromium effluent is a rapid process. Indeed, at pH 7 and at room temperature, the adsorption equilibrium is reached after 120 min and the kinetics follow a pseudo second order model. The adsorption isotherm is in good agreement with the Langmuir model. The results show that retention of Cr(VI) by LDH is by adsorption to the outer surface and by intercalation between the layers of LDH via the anionic exchange reactions. Removal of Cr(VI) was confirmed by the XRD results (increasing interlamellar distance) and those of IR spectroscopy (appearance of characteristic bands). The percent removal of chromium VI by LDH reached 99.7% for LDH/CrO_4 mass ratio equal to 3 with a maximum amount retained of 247,86 mg/g as ions CrO_4^{2-} ions.

Keywords: Chromium VI removal; Anionic clays; Kinetic study; Adsorption; Intercalation.

1. Introduction

The chromium ions have a very high toxicity [1], namely their carcinogenic, mutagenic, irritating and corrosive effects [2]. By its mobility and high solubility in water, Cr(VI) is 500 times more toxic than Cr(III) [3]. The huge world production of chromium VI each year [4] and the lack of treatment of industrial waste containing chromium show the increase in this problem (Fig. 1).

It is known that chromium (Cr) is a major pollutant in wastewater but has widespread application in industries like tanning, electroplating, pigments, textiles, alloys etc. The increased usage and inadequate disposal of chromate is a serious problem that we are facing in environmental perspective. Chromate has been known to be carcinogenic by inhalation, corrosive to tissue, sources of skin dermatitis problems, liver damage, etc. Cr(VI) is one of the most dangerous heavy metals because of its strong oxidizability and high toxicity [5,6], it is more water soluble, easily enters into living cells, and is much more toxic than Cr(III) which is essential for humans [7]. Moreover, Cr(VI) exhibits high mobility in most neutral to alkaline soils; it poses a great threat to surface water and groundwater [8].

Different methods for the removal of toxic Cr(VI) involve chemical precipitation, electrolysis, biochemical process and adsorption [9-12].

Ait Bentaleb et al.

Layered double hydroxides (LDH) offer a large interlayer surface with a host of diverse exchangeable anionic species, giving it high removal efficiency of anionic contaminants. LDH play an important role in medicine, removal of pesticides, biological material science, etc.
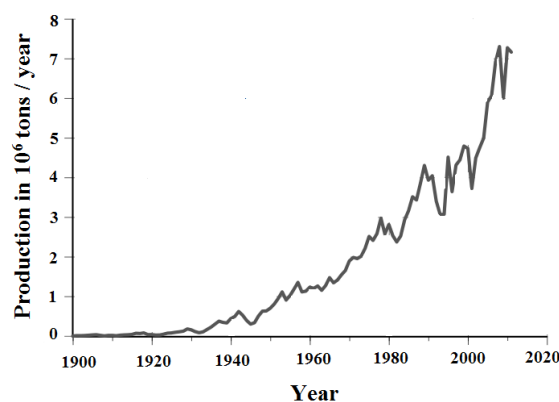
Figure 1: World production trend of chromium

LDH are considered among the most promising inorganic functional materials, due to their special layered structure, large surface area and low cost. Their general formula can be normally expressed as $[M^{II}_{1-x}M^{III}_x(OH)_2]^{x+}[(A^{n-}_{x/n}), mH_2O]$, where M^{II} and M^{III} are divalent and trivalent metal cations that occupy octahedral sites in the hydroxide layers, A^{n-} is an exchangeable anion located in the interlayer space between two hydroxide layers (Fig. 2).
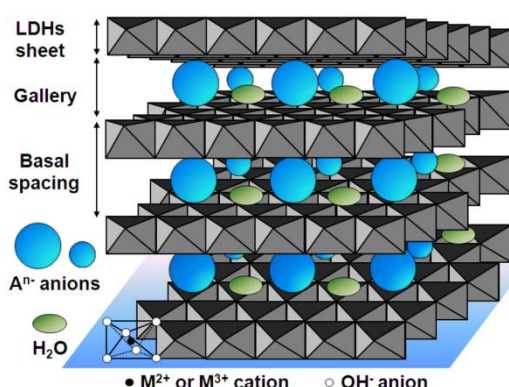
Figure 2: Schematic representation of LDH phase

2. Materials and methods
2.1. Adsorbent preparation and characterization

All experiments were carried out under a stream of N_2 to avoid, or at least minimize contamination by atmospheric CO_2. The [Zn-Al-Cl] LDH, with a [Zn]/[Al] ratio of 2, was synthesized by coprecipitation at a constant pH of 9.0 and at room temperature (25°C). Mixtures of molar $ZnCl_2$ and $AlCl_3$ aqueous solutions were slowly introduced into the reactor where the pH was maintained constant by the simultaneous addition of a 10^{-1}M NaOH solution. The resulting slurry was then stirred for 72 h at room temperature (25°C).

The precipitate was filtered, washed several times with decarbonated water and then dried at room temperature (25°C).

Characterization of the solid obtained by XRD (Fig. 3) showed that the phase corresponds to a pure LDH [13]. The solid consists of a well-crystallized single phase with large constituting crystallites. The lattice parameters refined on the hexagonal setting with a rhombohedral symmetry (space group: R-3m) and the experimental metal ratios are given in Table 1.

Table 1: Experimental [Zn]/[Al] ratio in the solid and its cell parameters

[Zn]/[Al]$_{th}$	[Zn]/[Al]$_{exp}$	**a** (nm)	**c** (nm)	**d** (nm)
2.00	1.99	0.307	2.334	0.778
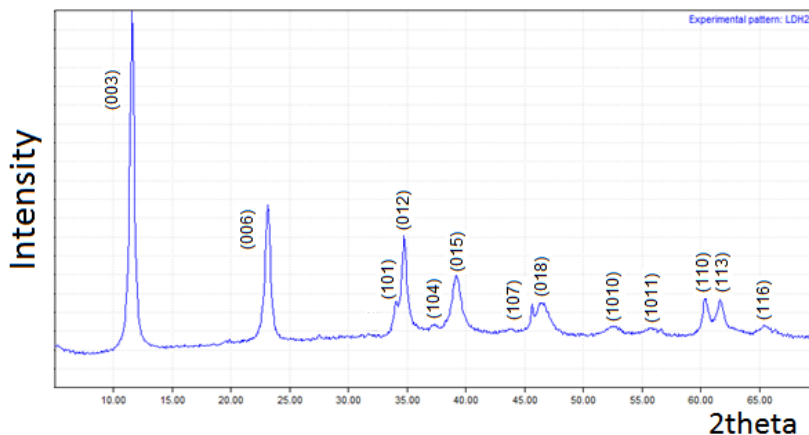
Figure 3: XRD pattern of [Zn-Al-Cl] precursor

2.2. Adsorbate

Chromium was prepared by dissolving the appropriate amount of potassium chromate K_2CrO_4 (Merck product > 99,5%) in decarbonated water. It can be assayed by several methods. In this study, we used the assay by UV-visible spectrophotometer after reaction with 1,5-diphenylcarbazide (DPC). It's a technique that is only applicable in highly acidic medium. Hexavalent chromium reacts with a total way with the DPC to form a highly colored complex in purple. Cr(VI) assay protocol is detailed by Dedkova *et al*. [14].

2.3. Retention experiments

Retention experiments were carried out by the batch equilibrium technique at room temperature (25°C), at constant pH, maintained by addition of NaOH, and under a stream of N_2. Amounts of [Zn-Al-Cl] were dispersed in 100 mL chromate solutions. The initial concentration of chromate was varied between 50 and 100 mg/L. After filtration, the solid products obtained were dried at room temperature before being analyzed by XRD and IR techniques. The supernatants were recovered and the residual dye concentration was determined by UV-Vis spectroscopy. The absorbance was measured at 540 nm on a Spectronic Genesys 20 spectrophotometer.

The Cr(VI) quantity retained by [Zn-Al-Cl], Q, was calculated as the difference between initial and equilibrium (final) concentrations of the dye in solution (C_i and C_e, respectively) by mass of the adsorbent (m) in the volume of solution (V) using the following equation:

$$Q = (C_i - C_e).V/m$$

2.4. Analytical techniques

The XRD equipment used was a Siemens D 501 diffractometer. Samples of unoriented powder were exposed to copper K_α radiation (λ= 0.15415 nm). Measurement conditions were 2h, range 5–70°, step size: 0.08-2h, and step counting time: 4s. Data acquisition was effective on a DACO-MP microcomputer. Unit cell constants were calculated using a least squares refinement.

Absorbance IR spectra were recorded on a Perkin-Elmer 16 PC spectrophotometer, at a resolution of 2 cm^{-1} and averaging over 100 scans, in the range 400–4000 cm^{-1}. Samples were pressed into KBr discs.

3. Results and discussion

Preliminary adsorption experiments were conducted to determine the optimal conditions for the retention of Cr(VI) on LDH regarding the pH value, contact time (t_c), initial concentration (C_i) of adsorbate and the mass ratio adsorbent/adsorbate.

3.1. Effect of pH
Generally pH of the aqueous solution is an important controlling parameter in the heavy metal retention process
and is considered to be an excellent parameter that controls the retention at water-adsorbent interfaces. 100 mg
of LDH was placed in 100 mL of dye solution with initial concentration 50 mg/L at 3 hours of contact time.
The retention of Cr(VI) by [Zn-Al-Cl] was studied at different pH values ranging from 4 to 11 (Fig. 4). The
maximum uptake levels of Cr(VI) were observed at pH between 7.0, which corresponds to the pH of natural
water. At lower pH values (<7), the low retention observed may be attributed to a partial dissolution of the basic
mineral matrix by acidic hydrolysis, which becomes more pronounced when the pH decreases. The low
adsorption observed at pH range 10–11 may be explained by a competition retention of Cr(VI) with the
carbonate ions for which the LDH is known to have a great affinity [13,15]. This hypothesis has been reported
in other works [16-19]. This phenomenon takes place despite the precautions taken during the preparation of the
solid sample and the kinetics study, when the pH value is high. Following these experiments, it was decided to
carry out the retention experiments at pH 7. It is well known that the dominant form of Cr(VI) at pH 7 is CrO_4^{2-}.
It can be concluded that the active form of Cr(VI) that can be adsorbed in this study is mainly CrO_4^{2-}.
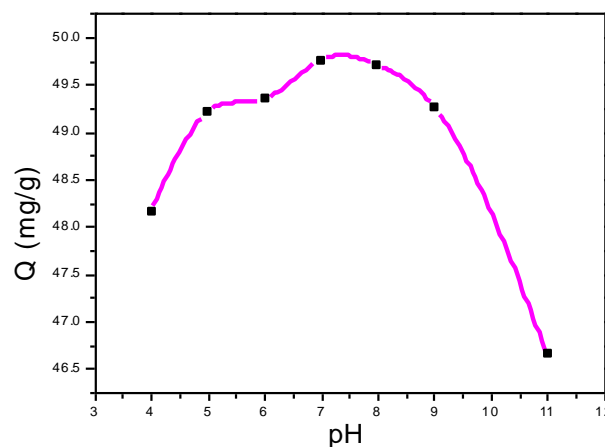
Figure 4: Amount of Cr(VI) retained by [Zn-Al-Cl] at different pH values

3.2. Effect of contact time (kinetic study)
In order to determine the equilibrium time value for the retention of chromium VI, retention was studied at pH
7.
The amount of Cr(VI) retained by [Zn-Al-Cl] as a function of contact time, using a constant adsorbent mass of
100 mg and different initial concentrations of chromium (VI) 50 and 100 mg/L in 100 mL solution, is shown in
Figure 5. The kinetic study shows that the retention equilibrium state is reached after a contact time of 2h since
no change in the retained amount is detected afterwards.
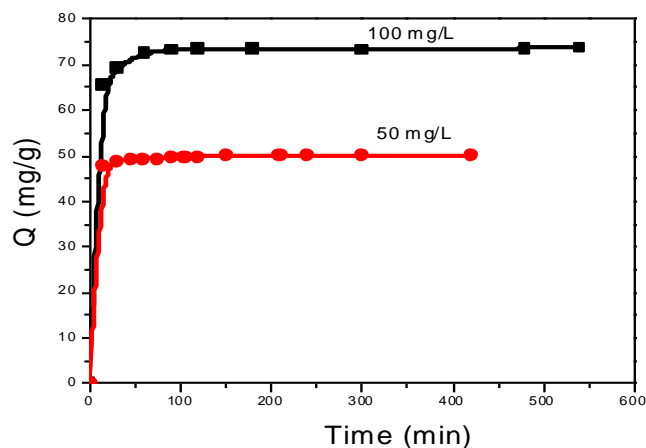
Figure 5: Amount of Cr(VI) sorbed by 100 mg of [Zn-Al-Cl] versus contact time at two different Cr(VI) initial
concentrations

To be sure that the equilibrium state is reached for higher concentration, a Cr(VI)-LDH contact time of 2 hours was applied in the retention experiments. Similar behavior was obtained for other adsorbates with LDH such Cr(III), phosphonates or dyes indigo carmine and methyl orange [18,21-23].

3.3. Adsorption isotherms
3.3.1. Langmuir isotherm
Figure 6 displays the retention isotherms of Cr(VI) onto 30, 60 and 100 mg of LDH. The chromium VI adsorption isotherms on [Zn-Al-Cl] can be considered clearly as pure L-type, indicating that the interaction sorbate–sorbent is much stronger than solvent–sorbent at the adsorption sites. Isotherms with this profile are typical of systems where the functional adsorbate is strongly attracted by the adsorbent, mostly by ion–ion interaction, which tends to reach a saturation value given by a nearly isotherm plateau. These results again suggest that chromate anions are preferentially removed.
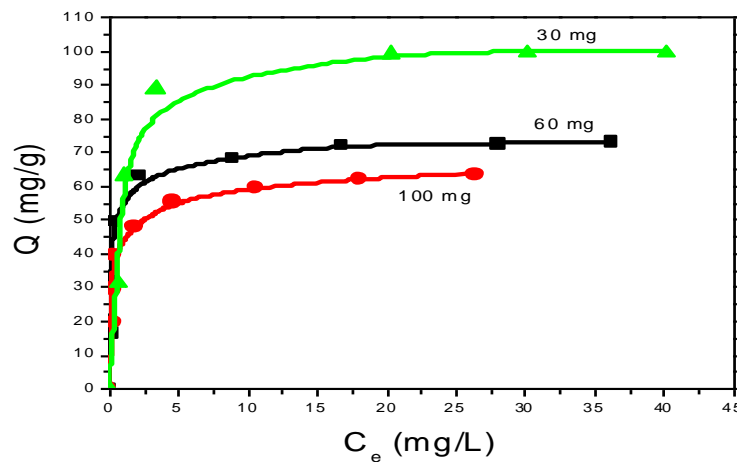
Figure 6: Adsorption isotherms of Cr(VI) on LDH at different adsorbent doses (30, 60 and 100 mg)

As may be seen, the Cr(VI) retention is inversely proportional to the mass of LDH. The Q_m value increases when the LDH mass decreases; this is somehow normal if we know that retention of Cr(VI) by the LDH can be done, in addition to adsorption, also by intercalation between the layers. This intercalation requires an increasing molar ratio (Cr(VI)/Cl) and therefore relatively small mass of LDH to allow maximum exchange of the chloride ions by the chromate ions.

The data for the uptake of Cr(VI) have been processed in accordance with the linear form of Langmuir isotherm equation:

$$C_e/Q = (1/KQ_m) + C_e/Q_m$$

Q is the quantity of Cr(VI) retained by the unit mass of LDH (mg/g); Q_m, the maximum quantity of Cr(VI) retained by the unit mass of LDH (mg/g); C_e, the equilibrium concentration of Cr(VI) (mg/L) and K is the affinity constant of Cr(VI) for LDH (L/mg).

A linear relationship was observed among the plotted parameters (Fig. 7), which indicates the applicability of the Langmuir equation. The sorption parameters obtained are summarized in Table 2.

These isotherms had an appearance reminiscent of those of the Langmuir adsorption isotherms. They provide a satisfactory linearization of retained amount, Q. This linearization was used to standardize the method of determining the maximum quantity Q_m. It also provides the affinity constant, K, on which it is difficult to pronounce. In that order of size, the K values are at least comparable, suggesting that whatever the LDH mass used, the type of interaction between adsorbent and adsorbate is the same. However, the maximum adsorbed amount decreases when the mass of LDH is increased.

3.3.2. Freundlich isotherm model
The accordance with the linear form of Freundlich equation is as follows:

$$Ln(q_e) = Ln(K_f) + 1/n \, Ln(C_e)$$

where q_e is the amount of metal ion sorbed at equilibrium per gram of adsorbent (mg/g), C_e the equilibrium concentration of metal ion in the solution (mg/L), K_f and n the Freundlich model constants. Freundlich

parameters K_f and n are determined by plotting Log q_e versus Log C_e. Figure 8 shows the linear plots of the Freundlich isotherm of Cr(VI) retention on LDH.
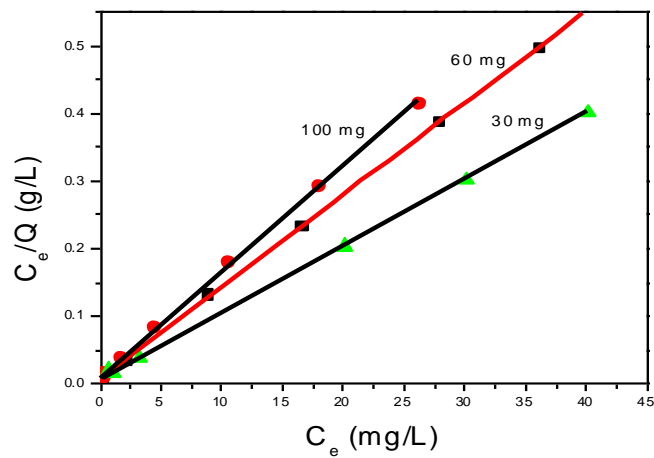
Figure 7: Linearization curves with three different sorbing doses (30, 60 and 100 mg)
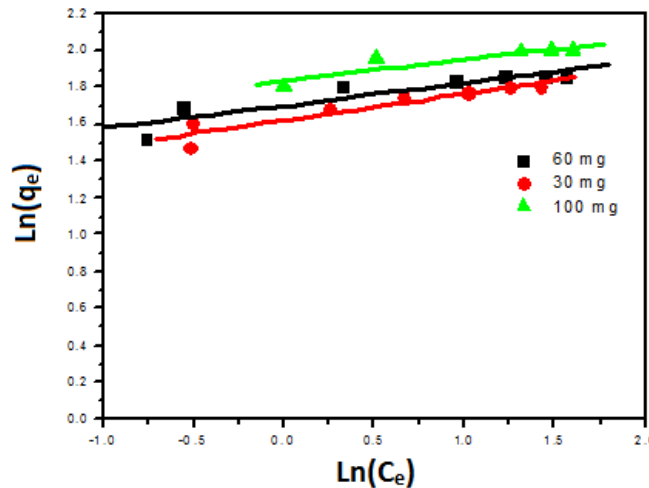
Figure 8: Linearized Freundlich isotherm plots of Cr(VI) adsorption
by three different LDH masses

The Langmuir and Freundlich equations were used in the analysis of the adsorption results.
Table 2 shows the comparing the two isotherm models described above; the value of correlation coefficient (R^2 = 0.999) indicates that the Langmuir isotherm was the most suitable for the characterization of Cr(VI) retention behavior. Q_m of Cr(VI) increases from 148.716 to 247.863 mg/g as chromate ions with the decrease of LDH mass (Table 2). It was found that LDH showed high capacity retention to Cr(VI). These results showed that the Langmuir isotherm model with results quite well, suggesting that the surface of the sorbent is homogeneous.

Table 2: Langmuir and Freundlich isotherm model constants and correlation coefficients
for retention of Cr(VI) on LDH

m_{HDL} (mg)	Langmuir isotherm				Freundlich isotherm			
	Q_m (mg/g) (CrO_4^{2-})	Q_m (mg/g) Cr(VI)	K (L/mg)	R^2	K_f (mg/g) (CrO_4^{2-})	K_f (mg/g) Cr(VI)	n	R^2
30	247.863	111.111	1.286	0.999	153.561	68.838	8.928	0.888
60	171.597	76.923	3.250	0.999	112.319	50.350	8.196	0.829
100	148.716	66.666	2.142	0.999	93.208	41.783	6.944	0.834

3.3.3. Adsorption Kinetics

It is known that the adsorption kinetics describes the order and the solute uptake rate governing the residence time of the adsorption reaction, is one of the most important characteristics that define the efficiency of adsorption. Figure 9 shows the kinetic of Cr(VI) adsorption onto LDH. The adsorption of Cr(VI) by LDH is fast. In such experimental conditions, most Cr(VI) in the form of chromate ions may be removed after 2 h. The above adsorption kinetic experimental data can be best fitted into a pseudo-second-order rate kinetic model. Different models were attempted to test the kinetics of interactions with LDH and chromate anions are expressed as follows:

$$\mathbf{ln\,(q_e - q_t) = ln\,q_e - k_1 t} \quad : \quad \text{pseudo-first order} \quad [24]$$
$$\mathbf{t/q_t = 1/(k_2 q_e^2) + (1/q_e)\,t} \quad : \quad \text{pseudo-second order} \quad [25]$$

where q_e and q_t are the amount of Cr(VI) adsorbed at equilibrium and at time t, respectively. k_1 and k_2 are the rate constants of the pseudo-first and pseudo-second order models of adsorption.

The pseudo second-order kinetic at different mass is plotted in Figure 9; k_2 and q_e calculated from the model are also listed in table 3 along with the corresponding correlation coefficient.

When second-order kinetics is applied, the t/q_t versus t plots are also linear and the second-order rate constant, k_2, is 0.007 and 0.012 g/mg.min for two mass concentrations 50 and 100 mg/L respectively (Table 3).

The predicted equilibrium uptakes were close to the experimental values indicating the applicability of the pseudo second-order model and the correlation coefficient values (R^2) suggests that this model represents the adsorption kinetics very well.
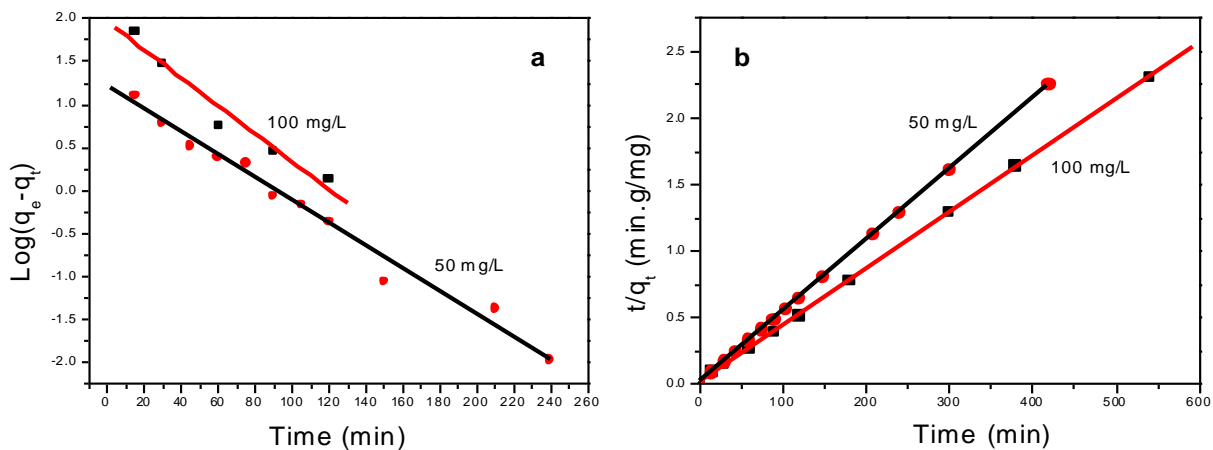
Figure 9: Pseudo-first order model (a) and pseudo-second order model (b) for the kinetic of Cr(VI) adsorption onto LDH

Table 3: Adsorption kinetics describes the order and correlation coefficients for retention of Cr(VI) by LDH

C_0 (mg/L)	pseudo-first order					pseudo-second order				
	Equation	k_1 (min^{-1})	$Q_{e\,th}$ (mg/g)	$Q_{e\,exp}$ (mg/g)	R^2	Equation	k_2 (g/mg.min)	$Q_{e\,th}$ (mg/g)	$Q_{e\,exp}$ (mg/g)	R^2
50	Log(q_e-q_t) = - 0.013.t +0.581	0.0299	3.810	49.838	0.972	t/q_t = 0.02.t+0.013	0.007	50	49.814	1
100	Log(q_e-q_t) = - 0.013.t +1.038	0.0299	10.914	73.692	0.958	t/q_t = 0.013.t + 0.015	0.012	76.923	73.269	0.999

3.3.4. Intra-particle diffusion

To investigate the contribution of intra-particle behavior on the adsorption process, the rate constant for intra-particle diffusion can be calculated from the following equation [26,27]:

$$Q_t = K_i\,t^{1/2} + C$$

where K_i is the intra-particle diffusion rate constant (mg/g), and C is the vertical axis intercept. If the plot of Q_t against $t^{1/2}$ were linear, the adsorption process was deemed to have been determined by the intra-particle diffusion step.

Additionally, intra-particle diffusion was the only rate-limiting step if the line tended to pass through the origin. Indeed, in recent work, these lines correspond to the existence of the external diffusion process (external surface adsorption), followed by intra-particle diffusion and finally to a slow diffusion of the adsorbate to the micropores of the adsorbent [28,29].

The intra-particle diffusion model adsorption Cr(VI) on the LDH is shown in Figure 10. It may be noted that the diffusion mechanism of adsorption system is described by two distinct regions instead of linear over the entire domain implying that the process has more than one step. The intermediate step would almost not evident. The parameter C (Table 4), which is proportional to the thickness of the double layer, increases with the Cr(VI) concentration is relatively large. Some authors have linked increased such value to the effect of growing the double layer on the adsorption, resulting in the predominance of the external diffusion of the intra-particle diffusion [30,31].
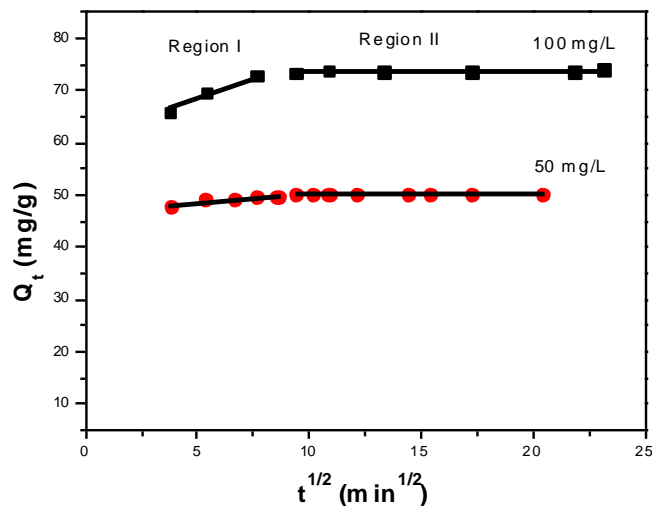
Figure 10: Intra-particle diffusion kinetic for adsorption of Cr(VI) ions on LDH

In a similar study on the elimination of Cr(VI) by hydrothermal synthetic layered double hydroxides [32], the authors considered that the diffusion mechanism of adsorption system can be described as two separate regions instead of linear over the entire domain implying that the process has more than one step.

Table 4: Rate constants for intra-particle diffusion

C_0 (mg /L)	Region I			Region II		
	K_{1P} (mg/g.min$^{1/2}$)	C_1 (mg/g)	R^2	K_{2P} (mg/g.min$^{1/2}$)	C_2 (mg/g)	R^2
50	0.270	46.94	0.926	0.002	49.78	0.970
100	0.79	61.41	0.890	0.066	72.01	0.986

3.4. Intercalation chromate ions
Study by X-ray diffraction
The XRD of the solids obtained by ion exchange of chloride by chromate correspond to that of a hydrotalcite-type material.
Figure 11 shows the XRD patterns for [Zn-Al-CrO$_4$] LDHs prepared with different mass ratios m_{LDH}/m_{CrO4}.
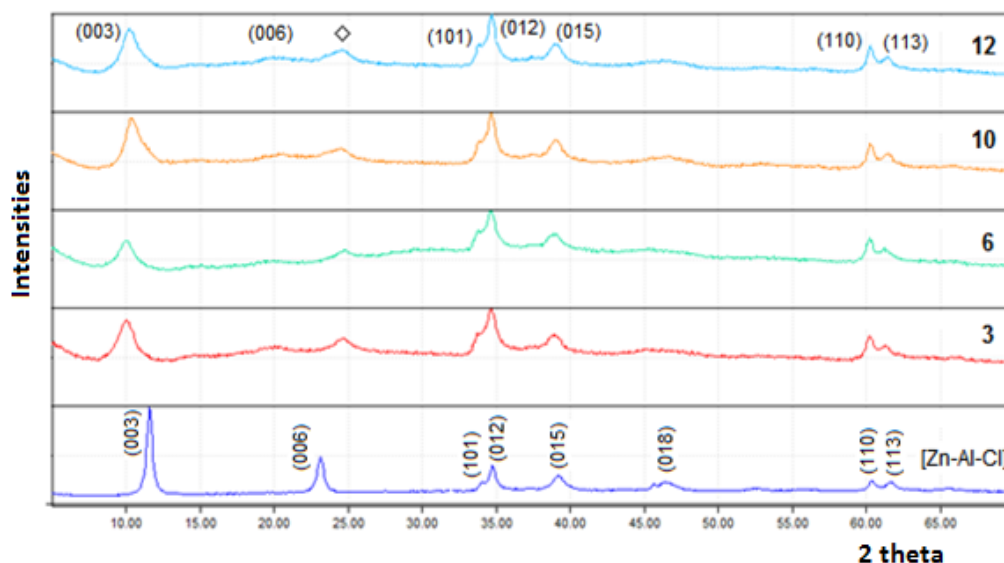
Figure 11: XRD patterns of the phases obtained after retention of Cr(VI) at different mass ratios m_{LDH}/m_{CrO4}

The layered structure of the material is preserved upon intercalation. However, the crystallinity is lowered, as attested by the broadening of the lines and the decrease in their intensity. In addition, intercalation is observed to cause a displacement of the (003) line, denoting an increase in the interlayer space which is due to the exchange of the chloride by the larger chromate ions [20]. Furthermore, the adsorption on the surface does not affect this distance for low concentrations of the Cr(VI). By contrast, for relatively high concentrations, increased interlayer distance means that there is an exchange between chloride ions and the anions of chromate, which are larger and accompanied by the maximum occupancy of the available anionic sites.

The cell parameters for the best compound, in terms of crystallinity, were **a** = 0.307 nm, **c** = 2.676 nm and the interlayer distance **d** = 0.892 nm.

3.5. Study by infrared spectroscopy

The IR spectra of the phases prepared (Fig. 12) are characteristic of [Zn-Al-Cl] LDH and [Zn-Al-CrO$_4$] after adsorption at different mass ratios are characteristic of LDH phases with the presence of bands reflecting the adsorption of CrO_4^{2-}.
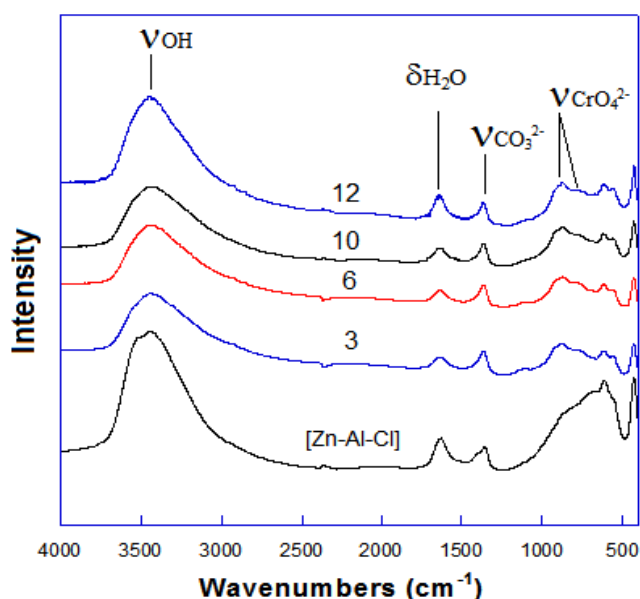
Figure 12: IR spectra of phases obtained after retention of Cr (VI) at different mass ratios m_{LDH}/m_{CrO4}

A high intensity band centered on 3460 cm^{-1} was observed, which could be attributed to the stretching vibration of O-H bonds in metal hydroxides and water molecules. The band appearing at 1628 cm^{-1} revealed the O-H bending mode of the water molecules. The bands revealed the presence of hydroxyl ions arising from the brucite-layers. The band at 1360 cm^{-1} was attributed to the characteristic vibrations of carbonate contamination. The bands at 809, 601 and 451 cm^{-1} are ascribed to the lattice vibration modes attributed to M–O and M–O–M vibrations [16]. After adsorption, the bands of 750 to 950 cm^{-1} correspond to characteristic stretching vibrations CrO_4^{2-} ions.

3.6. Structural model
In the light of these results, we can confirm that the chromate anion is intercalated in the interlayer space and bound to the host matrix by hydrogen bonding with an interlayer distance of 0.892 nm. Knowing the thickness of the brucite-like layer (e = 0.21 nm), the hydrogen bond distances between guest and host ($d_{H—O}$ = 0.27 nm) and we determined the value of the length of the CrO_4^{2-} anion by molecular orbital semi-empirical method with the Gaussian 03 software, the calculated value is 0.1601 nm. We proposed an orientation of the anion chromate between the layered double hydroxide sheets.
Figure 13 shows the orientation of CrO_4^{2-} intercalated between layers of LDH.
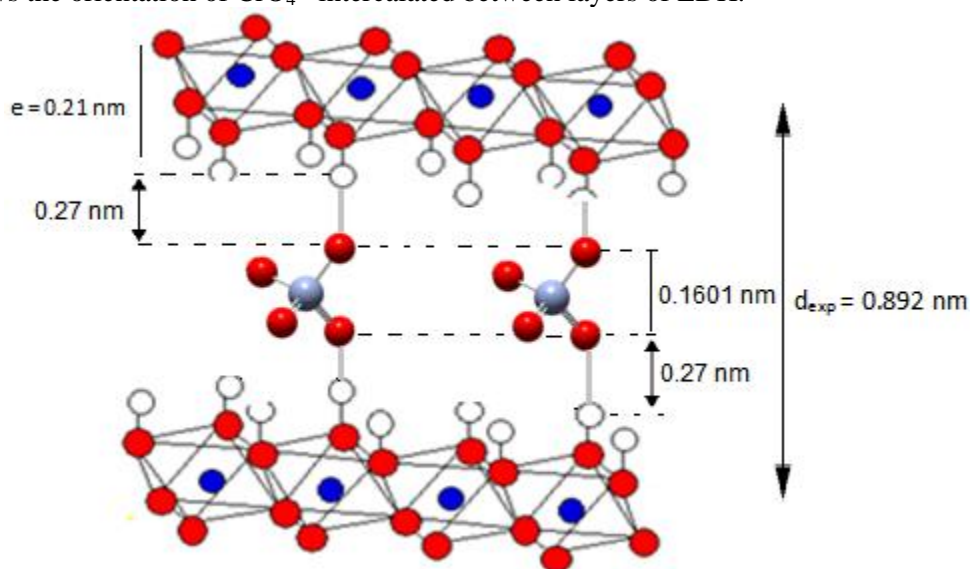
Figure 13: Schematic representation proposed for phase [Zn-Al-CrO$_4$]

The interlamellar distance determined experimentally, that is 0.892 nm, suggesting a direction of the anion in the interlayer space CrO_4^{2-}:

d = 0,21 + 0,27 + 0,27 + 0.1601 = 0,910 nm ~ 0,892 nm.

The fact that the experimental value is slightly less than the calculated one is probably due to electrostatic interactions between the anions and the layers. The water molecules are always present in the interlayer domain. In our case they take place between the chromate anions because they do not impose the interlamellar distance under our experimental conditions.

Conclusion

The affinity of anionic clays for CrO_4^{2-} anion was studied as a function of contact time, pH of solution and mass ratio of [Zn-Al-Cl]/CrO$_4$.
The removal of chromium effluent is a rapid process. Indeed, at pH 7 and at room temperature, the adsorption equilibrium is reached after 120 min and the kinetics follow a pseudo second order model.
The adsorption isotherm is in good agreement with the Langmuir model. Removal of Cr(VI) was confirmed by the XRD and IR results. This results show that retention of Cr(VI) by LDH is governed by adsorption to the outer surface and by intercalation between the layers of LDH via the anionic exchange reactions.
The percent removal of chromium VI by LDH reached 99.7% for LDH/CrO$_4$ mass ratio equal to 3 with a maximum amount retained of 247,86 mg/g as ions CrO_4^{2-}.

References

1. Shakoori A.R., Makhdoum M., Haq R.U., *Appl. Microbiol. Biotechnol*., 55 (2000) 348-351.
2. Karthikeyan T., Rajgopal S., Miranda I.R., *J. Hazard. Mater.,* 124 (2005) 192-199.
3. Kowalski Z., *J. Hazard. Mater.,* 37 (1994) 137-144.
4. Papp J.F. "Mineral Yearbook 2015: Chromium", United States Geological Survey.
5. Kotaś, J., Stasicka Z., *Environ. Pollut.*, 107(3) (2000) 263-283.
6. Ramos-Ramírez E., Ortega N.L.G., Soto C.A.C., Gutiérrez M.T.O., *J. Hazard. Mater*., 172(2-3) (2009) 1527-1531.
7. Kowalski Z., *J. Hazard. Mater.,* 37 (1994) 137-141.
8. Burrows D., in D. Burrows (Ed.), Chromium Metabolism and Toxicity, CRC Press, Boca Raton, FL (1983) p.138.
9. Gao H., Liu Y.G., Zeng G.M., Xu W.H., Li T., Xia W.B., *J. Hazard. Mater*., 150(2) (2008) 446-452.
10. Yalçin S., Apak R., Hizal J., Afşar H., *Sep. Sci. Technol*., 36(10) (2001) 2181-2196.
11. Nthumbi R.M., Ngila J.C., Moodley B., Kindness A., Petrik L., *Phys. Chem. Earth*, 50-52 (2012) 243-251.
12. Xiulan S. and Yuhong W., *Bull. Korean Chem. Soc.*, 35(6) (2014) 1817-1824.
13. Miyata S., *Clays Clay Miner.,* 23 (1975) 369-381.
14. Dedkova V.P., Shvoeva O.P., Savvin S.B., *J. Anal. Chem.*, 68 (2013) 117-122.
15. Rey F., Forne´s V., Rojo J.M., *J. Chem. Soc. Faraday Trans*., 88 (1992) 2233-2238.
16. Legrouri A., Lakraimi M., Barroug A., De Roy A., Besse JP., *Water Res.*, 39 (2005) 3441-3448.
17. Lakraimi M., Legrouri A., Barroug A., De Roy A., Besse JP., *Mater. Res. Bull*., 41 (2006) 1763-1774.
18. EL Gaini L., Sebbar E., Boughaleb Y., Bakasse M., Lakraimi M., Meghea M., *Nonlinear Opt. Quantum Opt.,* 00 (2008) 1-13.
19. El Khattabi E., Lakraimi M., Badreddine M., Legrouri A., Cherkaoui O., Berraho M., *Appl. Water Sci.*, 3 (2013) 431-438.
20. Rubino FM., *J. Chromatogr. B Biomed. Sci. Appl.*, 764(1-2) (2001) 217-254.
21. Lahkale R., Sadik R., Sebbar E. *J. Mater. Environ. Sci.,* 5 (S2) (2014) 2403-2408.
22. El Gaini L., Lakraimi M., Sebbar E., Meghea A., Bakasse M., *J. Hazard. Mater*., 161 (2009) 627-632.
23. Elkhattabi E., Lakraimi M., Berraho M., Legrouri A., Hammal R., Badreddine M., El Gaini L., *J. Mater. Environ. Sci.*, 7(3) (2016) 790-798.
24. Ho Y.S., Mckay G., *Water res*., 34(3) (2000) 735-742.
25. Cheung W.H., Szeto Y.S., Mckay G., *Bioresour. Technol.*, 98(15) (2007) 2897-2904.
26. Yang Y.Q., Gao N.Y., Chu W.H., Zhang Y.J., Ma Y., *J. Hazard. Mater*., 209-210 (2012) 318-325.
27. Kang D.J., Yu X.L., Tong S.R., Ge M.F., Zuo J.C., Cao C.Y., Song W.G., *Chem. Eng. J*., 228 (2013) 731-740.
28. Choy K.K., Ko D.C., Cheung C.W., Porter J.F., McKay G., *J. Colloid Interf. Sci.*, 271(2) (2004), 284-295.
29. Ofomaja A.E., *React. Funct. Polym.*, 70(11) (2010) 879–889.
30. Vimonses V., Jin B., Chow C.W.K., Saint C., *J. Hazard. Mater*., 171(1-3) (2009) 941-947.
31. Özcan A.S., Erdem B., Özcan A., *Colloid Surface A*, 266 (1-3) (2005) 73-81.
32. Wang W., Zhou J., Achari G., Yu J., Cai W., *Colloid Surface A*, 457 (2014) 33-40.

(2016) ; www.jmaterenvironsci.com